Transportation Research Part D 120 (2023) 103774

Contents lists available at ScienceDirect

Transportation Research Part D

journal homepage: www.elsevier.com/locate/trd

Developing an official program to calculate heavy-duty vehicles CO_2 emissions in Korea

Jigu Seo [a], Sungwook Park [b,*]

[a] Graduate School of Hanyang University, 222 Wangwimni-ro, Seongdong-gu, Seoul 04763, Republic of Korea
[b] Department of Mechanical Engineering, Hanyang University, 222 Wangwimni-ro, Seongdong-gu, Seoul 04763, Republic of Korea

ARTICLE INFO

Keywords:
Heavy-duty vehicle emission simulator
Longitudinal vehicle dynamics
Vehicle system model
Greenhouse gas emission
Fuel efficiency

ABSTRACT

In 2020, Korean government introduced a CO_2 monitoring regulation that heavy-duty vehicle (HDV) manufactures are required to submit CO_2 calculation data using Heavy-duty vehicle Emission Simulator (HES). Based on HES program, the mandatory CO_2 regulation for HDVs is expected to be implemented from 2026. This study addresses the development of HES program, which is a vehicle dynamics-based vehicle system model that estimates fuel consumption and CO_2 emissions of HDVs. The CO_2 prediction accuracy of HES was rigorously validated with 19 experimental data, and the average CO_2 emission error between the experimental values and HES results was 4.6%. For comparative analysis between HES and European HDV simulation program VECTO, 21 simulations were performed using the same input data for both programs, and the average CO_2 emission error is 1.59%. Using the HES program, we calculated CO_2 emissions from HDVs from 2015 to 2020 in Korea.

1. Introduction

The average global mean surface temperature has risen by about 1.0 °C above pre-industrial levels due to global warming (Masson-Delmotte et al., 2018). Global warming causes many serious problems, including climate change, sea level rise, as well as risks to biodiversity and ecosystems (Bernstein et al., 2008, Pachauri et al., 2014). The international community recognized the seriousness of climate change and adopted the Kyoto Protocol in 1997, which imposed obligations on developed countries to reduce greenhouse gas (GHG) emissions from the year 2005 (Grubb et al., 1999). In the year of 2015, the Paris Agreement was adopted by 195 Parties, at the 21st Conference of the Parties (COP21) of the United Nations Framework Convention on Climate Change (UNFCCC) to replace the Kyoto Protocol, which expired in 2020 (Rogelj et al., 2016). In October 2018, the Intergovernmental Panel on Climate Change (IPCC) proposed the pathways for GHG emissions to limit global warming to 1.5 °C (Masson-Delmotte et al., 2018). This report provided

Abbreviations: ADVISOR, Advanced Vehicle Simulator; CNG, compressed natural gas; CO_2, carbon dioxide; COP, Conference of the Parties; CVS, constant volume sampling; GEM, greenhouse gas emission model; GHG, greenhouse gas; HDV, heavy-duty vehicle; HES, heavy-duty vehicle emission simulator; IPCC, international panel on climate change; K-WHVC, Korean-world harmonized vehicle cycle; LDV, light-duty vehicle; NIER, National Institute of Environmental Research Korea; OBD, on-board diagnostics; PEMS, portable emission measurement system; PHEM, passenger car and heavy-duty emission model; PTO, power take off; UNFCCC, United Nations Framework Convention on Climate Change; VECTO, vehicle emission calculation tool; VeTESS, vehicle transient emission simulation software; VKT, vehicle kilometers traveled.

* Corresponding author at: Department of Mechanical Engineering, Hanyang University, 17 Haengdang-dong, Seongdong-gu, Seoul 133791, Republic of Korea.
E-mail address: parks@hanyang.ac.kr (S. Park).

https://doi.org/10.1016/j.trd.2023.103774
Received 28 July 2022; Received in revised form 6 March 2023; Accepted 4 May 2023
Available online 11 May 2023

scientific evidence for the target of Paris Agreement of limiting the temperature rise below 1.5℃. According to the report, CO_2 emissions should be reduced by 45% from 2010 levels by 2030. In addition, CO_2 emissions due to human activities should be net zero by 2050.

Transportation is one of the biggest sources of GHG emission, which accounts for 15% of global GHG emissions (Pachauri et al., 2014), Since most of the current transportation is operated using petroleum, large portions of GHGs are emitted. To reduce GHG emissions due to this sector, various measures have been implemented such as deployment of eco-friendly vehicles, use of low-carbon fuels, and optimization of traffic systems. Among other methods, GHG emissions and fuel efficiency regulations for light-duty vehicle (LDVs) have been introduced in many countries, including the European Union, United States, Japan, Canada, China, India, Brazil, Saudi Aribia, Mexico, and South Korea (Miller et al., 2017; Yang and Bandivadekar, 2017). Globally, about 80% of new LDVs are subject to GHG and fuel efficiency regulations.

Currently, GHG regulations for heavy-duty vehicles (HDVs) have been introduced in many countries including the United States, the European Union, Canada, Japan, and China. In contrast to LDVs, GHG regulations for HDVs are in the early stages (Sharpe and Muncrief, 2015, Siskos and Moysoglou, 2019). In the United States (Sharpe et al., 2018) and Japan, GHG emission regulations for HDVs were implemented in 2014 and 2015, respectively. In 2019, the certification of the HDV CO_2 emissions in the European Union started. In addition, a monitoring regulation that assessed the existing GHG emissions of European HDVs was implemented (European Commission, 2018). The mandatory GHG standards for European HDVs will come into effect in 2025, and stricter GHG standards will be applied from 2030 (European Commission, 2019). In 2020, Korean government introduced a CO_2 monitoring regulation that HDV manufactures are required to submit CO_2 emission data of HDVs sold in Korea from 2021 to 2022 (ME, 2019). The purpose of monitoring regulation is to calculate the baseline CO_2 emissions of HDVs in Korea. Subsequently, Korean government has set a voluntary CO_2 reduction period from 2023 to 2025, with reduction targets are set at 2% for 2023, 4.5% for 2024, and 7.5% for 2025. During the voluntary reduction period, credits will be provided to manufactures that exceed their CO_2 reduction targets, and no penalties will be imposed for regulatory non-compliance. The mandatory reduction is expected to be implemented from 2026.

The distinction between GHG regulations for HDVs and LDVs relies on the method of testing. Chassis dynamometer tests are widely used in many countries to measure CO_2 emissions and fuel efficiency of LDVs (Triantafyllopoulos et al., 2019; Tutuianu et al., 2015). In the chassis dynamometer test, the vehicle follows the predefined target velocity in a laboratory under controlled conditions. The roller of the chassis dynamometer, which is in contact with the vehicle tire, applies rotational resistance force based on the road load coefficient of vehicle.

In contrast to LDVs, simulation methods are used to evaluate CO_2 emissions of HDVs in the United States, European Union, Japan, and South Korea. Since HDVs are considerably diverse compared to LDVs, it is costly and ineffective to measure GHG emissions of various vehicle families of HDVs using experimental methods. There are various axle configurations of HDVs such as 4X2, 4X4, 6X2, 6X4, and 8X2. Various tractor-trailer combinations and cargo bed customizations can also be obstacles to introducing the chassis dynamometer test for HDVs. Therefore, the simulation method has been used instead of the chassis dynamometer test to estimate the GHG emissions of HDVs. The United States developed the Greenhouse Gas Emissions Model (GEM) to calculate HDV CO_2 emissions (Newman et al., 2015; EPA GEM Phase2 V4.0). GEM phase 1 was released in 2011 and an updated version, GEM phase 2, was released in 2015. In Europe, the Vehicle Emission Calculation Tool (VECTO) was introduced in 2017 (Fontaras et al., 2013b; Zacharof et al., 2017). Both GEM and VECTO calculate CO_2 emissions and fuel consumption of HDVs based on vehicle dynamics and component modeling of the vehicle system.

In terms of CO_2 emissions and fuel consumption estimation, vehicle dynamics is an effective tool for analyzing the operating conditions of the vehicle and engine because fuel consumption and CO_2 emissions are highly correlated with the status of the engine and the vehicle. The Passenger car and Heavy-duty Emission Model (PHEM) estimates instantaneous vehicle emissions based on engine speed and load demand during a predefined driving pattern (Hausberger, 2009). PHEM accounts for most of the variables that affect fuel consumption, including driving resistance, internal transmission losses, gear shifting, and power consumption of auxiliaries. By considering these variables, PHEM calculates instantaneous engine speed and engine torque. Then, fuel consumption and emissions are interpolated from the engine map, which represents fuel consumption or emission as a function of the engine speed and engine torque. Vehicle Transient Emissions Simulation Software (VeTESS) calculates fuel consumption and emissions in a manner similar to PHEM (Beevers and Carslaw, 2005, Carolien et al., 2007). VeTESS calculates the external driving resistance such as aerodynamic drag, rolling resistance, acceleration resistance, and inclination resistance based on longitudinal vehicle dynamics. In addition to the external resistance forces, the vehicle system model considers the internal energy losses and gear shifting to calculate the engine operating conditions. The engine module calculates the fuel consumption and emissions using an emissions map, which represent specific emission values according to various engine operating conditions. Sun et al. (2021) estimated vehicle energy consumption based on vehicle simulation program Advanced Vehicle Simulator (ADVISOR). They analyzed the relationship between energy consumption and vehicle parameters such as vehicle body, transmission, battery, and tire.

In South Korea, the Heavy-duty vehicle Emission Simulator (HES) was developed for CO_2 emission certification of HDVs. HES was first introduced in 2016 (Seo et al., 2016), and we developed this program in corporation with Korean ministry of environment. In the early stage of HES development, the Korean government considered using VECTO as CO2 certification tool in Korea, instead of developing a new modeling platform, because most of HDVs sold in Korea were produced by domestic and European manufacturers. However, the Korean government decided to develop the HES program because it is difficult to apply VECTO to Korean regulations due to different HDV characteristics between the EU and Korea such as vehicle types, vehicle classification, driving pattern, etc. Instead, research has been conducted to increase the correlation between HES and VECTO during the HES development process.

HES is based on longitudinal vehicle dynamics and component modeling similar to VECTO and GEM. This simulation model calculates the dynamic conditions of the vehicle and engine operating conditions, such as engine speed and engine torque, by

simulating driving. Since the fuel consumption of vehicles are closely related to the operating conditions of the engine, the calculated engine operating conditions are used to predict fuel consumption using a fuel map, which represents the fuel consumption as a function of engine speed and engine torque. To simulate vehicle driving, various input data are required such as vehicle weight, tire radius, aerodynamic drag coefficient, rolling resistance force, gear ratio, etc. This study describes the development of HES including the modeling method and prediction accuracy validation. In addition, the annual CO_2 emissions between the year 2015 and 2020 were estimated to understand the current status of CO_2 emissions from Korean HDVs by integrating the simulation results and national statistical data on annual vehicle mileage and vehicle registration statistics.

2. Methodology

2.1. Modeling approach

HES estimates the vehicle's fuel consumption and CO_2 emissions by calculating the energy consumed for driving. Using longitudinal vehicle dynamics and vehicle system modeling, the energy required for driving was analyzed based on the longitudinal movement of a vehicle such as acceleration, cruising, and braking. Longitudinal vehicle dynamics is mainly concerned with the external forces acting on a vehicle such as rolling resistance force, aerodynamic drag force, and inclination force. The main interest of vehicle system models is internal vehicle factors such as gear shifting, transmission efficiency and internal energy losses, which affect the transmission of power from the engine to the wheel.

HES is a backward-looking simulator in which the vehicle follows the predefined target speed without a driver module. When the vehicle follows the target speed, the load acting on the wheel can be calculated based on longitudinal vehicle dynamics. Then, the vehicle system model analyzes the operating conditions of sub-components from the wheel to the engine. Using the engine operating conditions, the fuel consumption and CO_2 emissions can be interpolated from the fuel consumption map. When vehicle cannot follow the predefined target speed, HES reduces the target speed until the vehicle can achieve the target speed. Then HES recalculated the operating conditions of vehicle and engine. This chapter presents the modeling method of HES.

2.2. Structure of HES

2.2.1. Longitudinal vehicle dynamics

Fig. 1 shows the external forces acting on a vehicle. These forces consist of a driving force, rolling resistance force, aerodynamic drag force, and inclination force (Gillespie, 1992). When the vehicle moves forward, sufficient driving forces need to be supplied to the vehicle to overcome the resistance forces such as rolling resistance, aerodynamic drag and inclination forces. The longitudinal force balance of a vehicle is as follows.

$$m\ddot{x} = F_{DF} + F_{DR} - F_{RF} - F_{RR} - F_{air} - mg \bullet sin(\theta) \tag{1}$$

Here, F_{DF}, F_{DR} are the driving forces at the front tire and rear tire [N]. F_{RF}, F_{RR} are the rolling resistance forces at front ties and real tire [N], F_{air} is aerodynamic drag force [N], m is vehicle mass [kg], g is gravitational acceleration [m/s^2], and θ is road grade []. For vehicle mass, the standard payload for CO_2 certification of vehicles has been set at 50% Typically, HDVs operate with either a full load (100% payload) or an empty load (0% payload). Therefore, the midpoint between these two conditions, 50% payload, has been decided as the standard loading condition for CO_2 certification.

Rolling resistance force (F_R) is caused by the deformation of the tire (Pacejka, 2005). Tires are made of elastic materials that continuously deform and recover during driving. These energy losses can be characterized by the following equation:

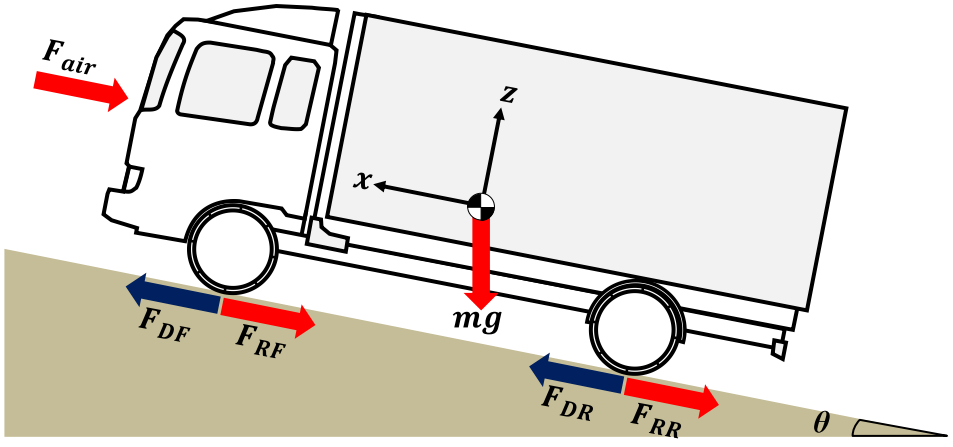

Fig. 1. Longitudinal external forces acting on the vehicle.

$$F_R = f_r \bullet F_z \tag{2}$$

Here, f_r is the rolling resistance coefficient [-], and F_Z is the vertical load [N].

Rolling resistance force is proportional to the rolling resistance coefficient and vertical load acting on the tire. The tire slip was neglected in this study. The rolling resistance coefficient is empirical value that can be measured from the experiment such as ISO 28580 (ISO 28580, 2009).

Aerodynamic drag force accounts for a major part of driving resistance, especially under high-speed driving conditions. For modern vehicles, more than half of the vehicle's fuel consumption under highway driving conditions is due to aerodynamic resistance (Sudin et al., 2014). Aerodynamic drag force (F_{air}) largely depends on vehicle speed and it can be characterized by the following semi-empirical equation:

$$F_{air} = 0.5 \bullet \rho \bullet C_d \bullet A \bullet v^2 \bullet k \tag{3}$$

Here, ρ is the air density $\left[kg/m^3\right]$, C_d is the air drag coefficient [-], A is the frontal area of the vehicle $\left[m^2\right]$, v is the vehicle speed [m/s], and k is the wind correction factor [-].

In this study, air density was assumed to be a constant value of 1.188 kg/m^3. The drag coefficient is a dimensionless coefficient, and the vehicle front area is a simple vehicle specification. The product of the two variables (CdA) is called drag area. CdA is an empirical value that can be measured from experimental tests (Gururaja, 2016). In Korea, both the constant speed test utilized in VECTO (European Commission, 2017) and the coast down test used in GEM (Environmental Protection Agency, 2016) are currently viable methods for measuring the air drag coefficient. It is expected that one of the two measurement methods will be selected as the standard air drag measurement method in Korea within the next few years. Wind correction factor is a speed-dependent correction factor that considers the influence of the wind angle. Cross wind correction model of VECTO (European Commission, 2021) was used to derive the correction factor. Depending on the vehicle types (truck, tractor, bus), predefined correction factors are used to calculate air drag force.

The driving force is the primary force that enables the vehicle to move. The source of driving force is the engine power, which is delivered to the wheel through the driveline. The relations between driving force (F_D) and wheel can be described as follows:

$$F_D = T_w / r_{eff} \tag{4}$$

$$r_{eff} = r_w \bullet 3/\pi \tag{5}$$

Here, T_w is the wheel torque [Nm], r_{eff} is the effective tire radius [m], and r_w is the tire radius [m].

The effective tire radius is the actual radius value when the wheel is rotating and a load is applied to the tire. Although the effective tire radius depends on various factors such as rotational speed, wheel load, thread depth, and composition of tire (Pacejka, 2005), a simple assumption (Lee et al., 2015) was used in this study. The tire radius r_w means the free radius when the load is not applied to the tire. Based on Eqs. (1) and (5), wheel torque (T_w) can be express in the following equation:

$$T_w = r_{eff} \bullet (m\ddot{x} + F_{RF} + F_{RR} + F_{air} + mg \bullet sin(\theta)) \tag{6}$$

Eq. (6) shows that the wheel torque can be calculated when the effective tire radius, vehicle weight, vehicle acceleration ($\ddot{x}$, $[m/s^2]$), rolling resistance force, aerodynamic drag force and road grade are known. In addition, the rotational speed of the wheel (ω_w, [rad/s]) can be calculated by following a simple equation:

$$\omega_w = v / r_{eff} \tag{7}$$

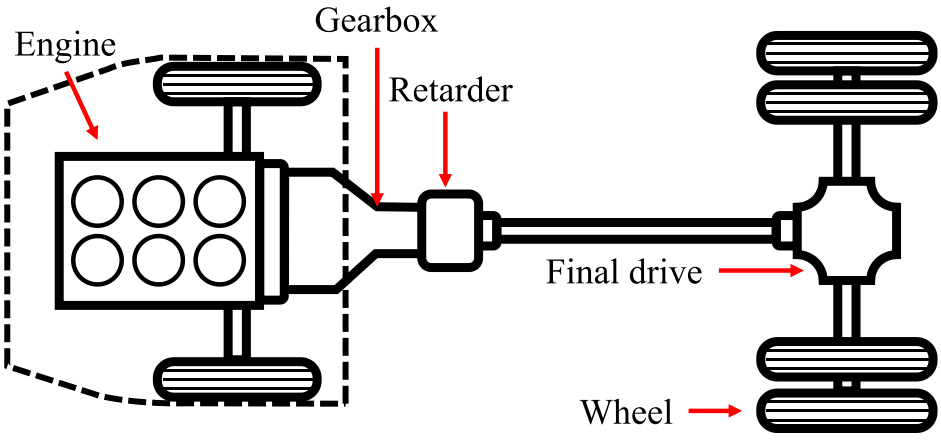

Fig. 2. Schematic diagram of a conventional heavy-duty vehicle.

The wheel torque and rotational speed of the wheel of vehicle can be calculated using Eqs. (6) and (7). Since the wheel is mechanically connected to the driveline of vehicle, the operating condition of vehicle sub-component can be calculated from the wheel to the engine. In the next section, a detailed description of the vehicle system model is presented.

2.2.2. Vehicle system model

Fig. 2 shows the major components of a driveline of HDV. The engine is the power source of the vehicle, which is closely related to fuel consumption and CO_2 emission. The power generated by the engine is transmitted to the wheel through the gearbox, retarder, and final drive. The actual transmitted power is reduced by the amount of transmission loss of the driveline. In addition, the gear ratios of the gearbox and final drive affect the relationship between the torque and rotation speed of each component.

The simplified structure of vehicle system is illustrated in Fig. 3. The power flows from the engine to the wheels. In contrast, the direction of the load is opposite to the power flow. According to the flow direction of power and load, there are two major modeling approaches for the vehicle system: a forward-looking vehicle model and a backward-looking vehicle model (Pettersson et al., 2020).

The calculation flow of the forward-looking model is similar to the power flow of the vehicle. In the forward-looking model, the driver module sends accelerator and brake pedal signals to the engine. Then, the power generated from the engine is delivered to the ground. When the engine power is not sufficient to achieve target velocity or the vehicle is moving faster than the target speed, the drive module modifies pedal signal to achieve target velocity within a tolerance. Since the forward-looking model uses a separate driver module to control the vehicle, the simulation model behaves likes an actual vehicle. In addition, various driver control algorithms such as predictive cruise control and advanced gear shifting algorithms can be implemented in driving simulations.

In contrast, the backward-looking model calculates engine power based on the required load from the wheel without driver module. Therefore, the calculation flow of the backward-looking model is from the wheel to the engine, which is similar to the load flow in Fig. 3. In contrast to the forward-looking model, driver module is not essential for the backward-looking model. Therefore, this modeling method is quite simple and stable.

Both forward-looking and backward-looking approaches have been widely used for the vehicle system model. These two approaches are often used in combination rather than individually. The European HDV CO_2 certification program VECTO is mainly based on the backward-looking approach (Fontaras et al., 2013a). However, VECTO also incorporates the forward-looking approach to its driver control module to implement eco-roll, look ahead coasting, and over-speeding control. The American HDV CO_2 certification program GEM is a forward-looking simulator in which the driver module constitutes a major part of the model (Newman et al., 2015). This model consists of four subsystems: driver, vehicle, powertrain, and ambient subsystem. In this study, backward-looking approach was used to develop HES.

2.2.2.1. Wheel module. Fig. 4 shows the schematic diagram of the input and output variables of wheel module. The input variables of wheel module are output variables of final drive module. As mentioned in Sec. 2.2.1, the rotational speed of wheel (ω_w) and wheel torque (T_w) can be calculated using Eqs. (6) and (7). The input variables of the wheel module can be calculated reversely using the following equations:

$$\omega_w = \omega_f \tag{8}$$

$$T_w = T_f - I_w \bullet \dot{\omega}_w \tag{9}$$

Here, ω_w is the rotational speed of wheel [rad/s], ω_f is the rotational speed of final drive [rad/s], T_w is the wheel torque [Nm], T_f is the final drive torque [Nm], I_w is the rotational inertia of the wheel [kg•m^2], and $\dot{\omega}_w$ is the angular acceleration of wheel [rad/s^2].

The input speed (rotational speed of final drive) and output speed (rotational speed of wheel) of the wheel module is same. However, the torque delivered through the wheel is reduced by the inertial losses. In HES, rotational inertia values are provided according to tire specifications as shown in Supplementary Table A.4.

2.2.2.2. Final drive module. The schematic diagram of the input and output variables of the final drive module is shown in Fig. 5. Rotational speed of final drive (ω_f), final drive torque (T_f) can be calculated as follows:

$$\omega_f = \omega_r / N_f \tag{10}$$

$$T_f = T_r \bullet N_f - T_{loss,f} \tag{11}$$

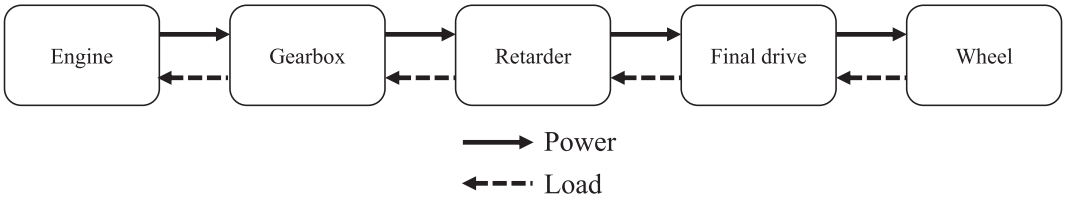

Fig. 3. The directions of power and load flows in a vehicle.

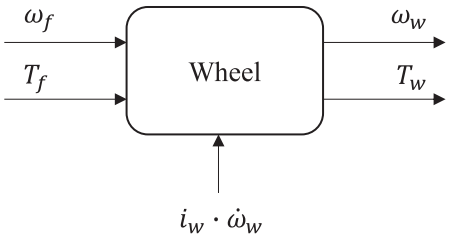

Fig. 4. Schematic of the wheel module.

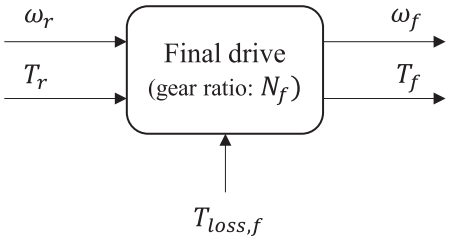

Fig. 5. Schematic of the final drive module.

Here, ω_r is the rotational speed of retarder [rad/s], N_f is the gear ratio of the final drive [-], T_r is the retarder torque [Nm], and $T_{loss,f}$ is the transmission loss in the final drive [Nm].

The rotational speed and torque are affected by the gear ratio as they pass through the final drive. In addition, the torque delivered through the final drive is reduced due to the transmission losses. Transmission losses of final drive is calculated by interpolating torque loss values from the final drive torque loss map, which is an empirical lookup table that represents torque loss as a function of the input torque and input speed. The map-based torque loss estimation function of HES is developed based on the European simulation model VECTO (Fontaras et al., 2013b).

2.2.2.3. Retarder module. The retarder module takes into account torque losses due to viscous drag forces. Fig. 6 illustrates the schematic diagram of the input and output variables of the wheel module. The rotational speed of retarder (ω_r), retarder drive torque (T_r) can be calculated as follows:

$$\omega_r = \omega_g \tag{12}$$

$$T_r = T_g - T_{loss,r} \tag{13}$$

Here, ω_r is the rotational speed of retarder [rad/s], ω_g is the rotational speed of the gearbox [rad/s], T_r is the retarder torque [Nm], T_g is the gearbox torque [Nm], and $T_{loss,r}$ is the transmission loss in the retarder [Nm].

The input and output rotational speeds of the retarder module are same. The amount of torque loss of retarder is interpolated from the retarder torque loss curve. The retarder torque loss curve is empirical data indicating torque loss as a function of the rotational

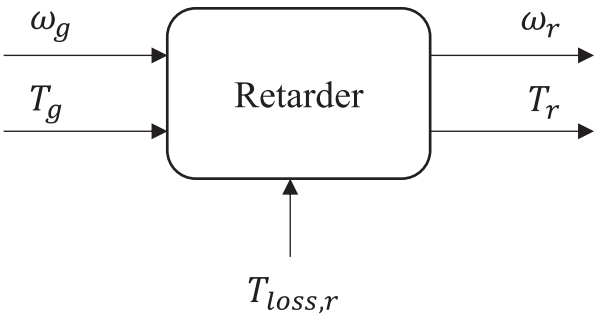

Fig. 6. Schematic of the retarder module.

speed of the retarder.

2.2.2.4. Gearbox module. The gearbox module is a major subsystem that determines gear shifting, which has a significant impact on the operating conditions of the engine. The schematic diagram of gearbox module is shown in Fig. 7. The rotational speed of gearbox (ω_g), gearbox torque (T_g) can be calculated as follows:

$$\omega_g = \omega_{eout}/N_g \tag{14}$$

$$T_g = T_{eout} \bullet N_g - T_{loss,t} \tag{15}$$

Here, $\omega_{e\,out}$ is the output rotational speed of engine [rad/s], N_g is the gear ratio of gearbox [-], $T_{e\,out}$ is the engine output torque [Nm], and $T_{loss,g}$ is the transmission loss in the gearbox [Nm].

The torque loss in the gearbox module was modeled in a manner similar to the final drive. Torque losses were interpolated from gearbox torque loss map that represents torque losses as a function of the input torque and input speed. In addition to the torque loss, the gear shifting algorithm determines the gear position based on the current engine speed (ω_e) and current engine torque (T_e). The upshifting is performed when the following conditions are satisfied.

Upshifting conditions:

- $\omega_e/\omega_{\max} >$ up shfit threshold
- $T_e/T_{\max} +$ torque reserve $< 100\%$
- $\text{Time}_{\text{after last shift}} > \text{Time}_{\text{up shift dealy}}\ [2\,\text{s}]$

One of the conditions for upshifting is that the normalized current engine speed must be higher than the threshold. The threshold for upshifting is different for each gear. The threshold and torque reserve values are predefined in HES, and user cannot change them. In addition, sufficient torque reserve is needed before upshifting. The upshift is restricted when the margin of torque is not sufficient. The last upshifting condition is the current time, which must be 2 s after the last shifting event. When the above three conditions are satisfied, the gearbox module shifts up a gear. The upshifting conditions can be seen in Fig. 8. Especially for HDVs that have more than a 7-speed gearbox, gear skipping for upshifting (+2 gears) is activated when the spare torque of the engine is sufficient. The torque reserve for gear skipping is higher than that of normal upshifting. In contrast to upshifting, engine torque is not considered in the determination of downshifting, and the conditions are simpler than those of upshifting. When the normalized engine speed is below the threshold for downshifting, the gearbox module decides to downshift as shown in Fig. 9. The threshold values for downshift is different for each gear, and these values are predefined in HES. Three gear shifting parameters (up shift threshold, torque reserve, and down shift threshold) were modified based on various cases of experimental data. The downshifting conditions depends on the current engine speed as follows:

Downshifting condition:

- $\omega_e/\omega_{\max} <$ down shfit threshold

2.2.2.5. Engine module. The engine is the source of vehicle power that fuel consumption and CO_2 emissions are closely related to the operating conditions of the engine. The schematic diagram of the input and output variables of the engine module is shown in Fig. 10. The output rotational speed of the engine (ω_{eout}) and engine output torque (T_{eout}) can be calculated as follows:

$$\omega_{eout} = \omega_e \tag{16}$$

$$T_{eout} = T_e - I_e \bullet \dot{\omega}_e - T_{aux} \tag{17}$$

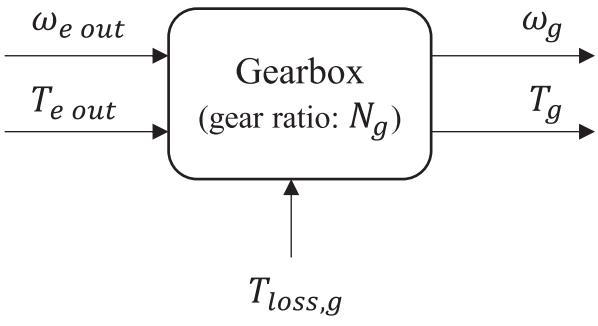

Fig. 7. Schematic of the gearbox module.

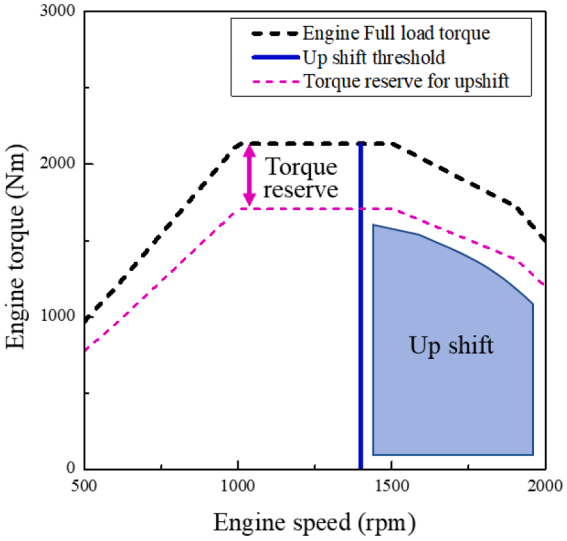

Fig. 8. Simplified diagram for upshifting conditions.

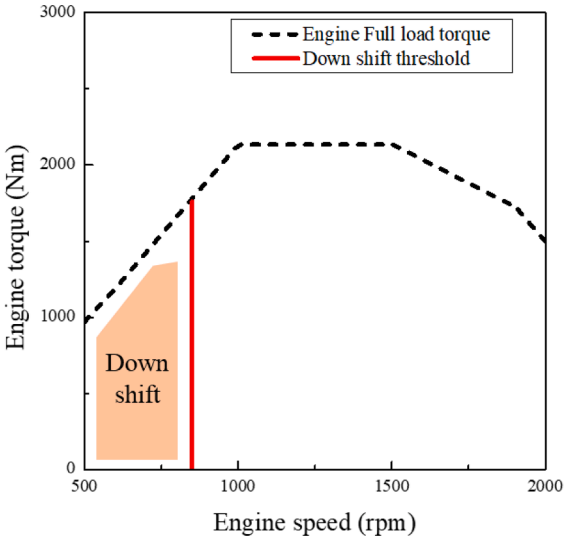

Fig. 9. Simplified diagram for downshifting conditions.

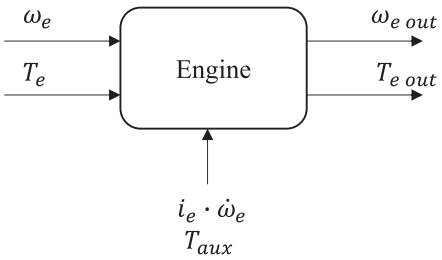

Fig. 10. Schematic of the engine module.

Here, ω_e is the engine speed [rad/s], T_e is the engine torque [Nm], I_e is the rotational inertia of engine [kg•m^2], $\dot{\omega}_e$ is the angular acceleration of engine [rad/s^2], and T_{aux} is the torque demand for auxiliaries [Nm]. HES determines the rotational inertia of the engine based on its displacement as shown in Supplementary Table A.5. In addition, it is expected that the Korean government will provide power consumption values for different types of auxiliaries.

Since the sub-component of vehicle is mechanically connected from the engine to the wheel, Eqs. (4) to (17) can be used to express the engine speed (ω_e) and engine torque (T_e) as follows:

$$\omega_e = v \bullet N_f \bullet N_g / r_{eff} \tag{18}$$

$$T_e = \left(\left(\left(F_d \bullet r_{eff} + I_w \bullet \dot{\omega}_w + T_{loss,\,f} \right) \Big/ N_f \right) + T_{loss,\,r} + T_{loss,\,t} \right) \Big/ N_g + I_e \bullet \dot{\omega}_e + T_{aux} \tag{19}$$

When the calculated engine torque exceeds the maximum engine torque, HES reduces the target speed until the vehicle can achieve the target speed within the torque limit. Then HES recalculated the operating conditions of vehicle and engine.

2.2.3. Fuel consumption and CO_2 emission calculation

The operating conditions of the engine are calculated at each time step using Eqs. (18) and (19). The fuel consumption can be interpolated using the calculated engine speed (ω_e) and engine torque (T_e) from a fuel consumption map, which is an empirical lookup table that represents the fuel consumption rate as a function of engine speed and engine torque. The engine fuel consumption map is derived from steady-state measurements using the fuel consumption mapping cycle utilized by VECTO (European Commission, 2017). In addition, since steady-state-based fuel consumption map has a limitation of not considering transient effects, HES corrects the fuel consumption values by applying the WHTC transient correction factors used by VECTO (European Commission, 2017). Fig. A.1 shows the example of fuel consumption map of a diesel engine with a displacement of 13,000 cc. Based on the user-defined fuel consumption map, HES calculate fuel consumption rate at each time step. After calculating fuel consumption, CO_2 emissions can be converted from fuel consumption using the carbon balance method. Typically, carbons contained in fuel are emitted into the atmosphere after the combustion in the form of CO_2, CO, and hydrocarbons. Therefore, the mass of carbons in fuel is equal to the carbon mass contained in the exhaust gas (Akita, 2014). By utilizing this relationship, fuel consumption can be converted to CO_2 emission. The Korean standard carbon balance method for diesel vehicle is expressed as follows (MOTIE, 2015).

$$FE_{dieselvehicle} = SW_{carbon} / (E_{CO_2}(0.273 + E_{HC} \cdot 0.858 + E_{CO} \cdot 0.429) \tag{20}$$

Here, $FE_{dieselvehicle}$ is the fuel economy [g/km], SW_{carbon} is the specific carbon weight of diesel fuel (Korean standard value: 707) [g/l], E_{CO_2} is the carbon dioxide emissions per kilometer [g/km], E_{HC} is the hydrocarbon emissions per kilometer [g/km], and E_{CO} is the carbon monoxide emissions per kilometer [g/km].

In this study, we assumed that all carbons in the fuel are oxidized to CO_2 and hydrocarbon and CO emissions are negligible. In addition, the Korean standard value for SW_{carbon} of diesel fuel is 707. Therefore, the carbons contained in 1 kg of diesel fuel are emitted as 3,146 g of CO_2, and this value was used as a CO_2-desel conversion factor in HES.

In addition to diesel fuel, natural gas is the second most widely used fuel for HDVs, and 3.64% of Korean HDVs use natural gas as fuel (MOLIT, 2021). Since natural gas is mainly composed of methane, the carbon weight fraction of natural gas is 0.756, and carbons in 1 kg of methane are emitted as 2,772 g of CO_2.

Table 1
Specifications of test vehicles.

NO.	Test method	Number of tests	Vehicle type	Fuel type	Engine displacement (L)	Maximum engine power (PS)	Vehicle Weight (kg)
Case 1	Chassis dynamometer test (K-WHVC)	3	Truck	Diesel	3.9	170	4,950
Case 2		1	Truck	Diesel	6.3	280	8,200
Case 3		2	Truck	Diesel	6.3	280	7,800
Case 4		2	Bus	Diesel	12.7	440	14,500
Case 5		3	Bus	CNG	11.7	290	13,500
Case 6	Real road driving test	1	Truck	Diesel	6.3	280	8,300
Case 7		1	Truck	Diesel	6.3	280	9,200
Case 8		1	Truck	Diesel	12.7	540	30,000
Case 9		1	Truck	Diesel	12.7	540	30,000
Case 10		1	Truck	Diesel	12.7	540	30,000
Case 11		1	Bus	Diesel	9.9	430	13,000
Case 12		1	Bus	Diesel	12.7	440	13,900
Case 13		1	Bus	Diesel	12.7	440	13,900

2.3. Vehicle experiment for HES validation

The prediction accuracy of HES was validated by comparing the simulation results with experimental results measured by National Institute of Environment Research (NIER), the national regulatory agency responsible for vehicle emissions. According to the Korean national statistics (MOLIT, 2021), trucks, buses, and tractors account for about 80%, 17% and 3% of the total HDVs, respectively. Depending on the type of fuel used, 96.4% of HDVs are powered by diesel engines and the remaining 3.6% HDVs are powered by natural gas engines (compressed natural gas, CNG). Considering the distribution of HDVs in Korea, thirteen HDVs were tested including a truck, bus, and a CNG-powered vehicle to verify the model performance for various types of HDVs. The specifications of the thirteen test vehicles are shown in Table 1.

Both chassis dynamometer tests and real road driving tests were conducted. In the chassis dynamometer test, vehicles were controlled to meet the target speed of predefined driving cycle (Fig. 11). In contrast, the velocity of vehicles in real road driving test were different in each test due to varying conditions of traffic signals, traffic volumes, and weather conditions. The measured speed and altitude data from the real road driving test (Fig. A.2) used as the driving conditions in the simulation.

During the experiment, the operating variables of the vehicle such as vehicle speed, road gradient, engine speed, and engine torque were measured through the on-board diagnostics (OBD) data logger. For the chassis dynamometer test, the constant volume sampling (CVS) method was used to sample the CO_2 emissions. In contrast, a portable emission measurement system (PEMS) was used to measure exhaust emissions in the real road driving test. Driving tests were conducted repeatedly two to three times for Case 1, Case 3, Case 4, and Case 5 vehicles. For example, the Case 1 vehicle was tested three times: Case 1–1, Case 1–2, and Case 1–3. Vehicles for Cases 1 through 5 were tested using a chassis dynamometer. CO_2 emissions for vehicles in Cases 6 through 13 were measured under real road driving conditions. Since chassis dynamometer test was conducted in flat condition, road gradient was not considered for HES validation based on chassis dynamometer test data. In contrast, road gradient was used to calculate CO_2 emissions under real road driving conditions.

We obtained the input data for the simulation from a government database. The Ministry of Environment manages engine test data and vehicle information for HDVs to regulate the pollutant emissions, and we used these data for simulation input. In addition, the air drag and rolling resistance coefficients were calculated based on Eqs. (22) and (23) in section 2.4.1. Although the present study verified the HES accuracy using approximated air drag and rolling resistance coefficients, future research will consider measured air drag and rolling resistance coefficients for HES validation.

2.4. Estimation of heavy-duty vehicle CO_2 emissions in Korea

Simulation method is effective in estimating fleet-wide CO_2 emissions of vehicles. Zacharof et al. (2021) estimated HDV fleet CO_2 emissions using VECTO simulation result. Depending on the sampling method, they investigated the method to accurately estimate fleet-level CO_2 emissions. In this study, CO_2 emissions of Korean HDVs from 2015 to 2020 were estimated by integrating simulation results and national statistical data. The simulation results of 375 HDVs and annual vehicle mileage statistics and vehicle registration statistics were used to assess the annual CO_2 emissions according to the following equation:

$$CO_2 emission[g/year] = \sum_i^n E_i \bullet VKT_i \bullet N_i \tag{21}$$

Here, i is the vehicle type index [-], E_i is the CO_2 emissions [g/km], VKT_i is the vehicle kilometers traveled [km/year], and N_i is the number of vehicles [-].

2.4.1. Simulation conditions

Specifications of 375 vehicles were used for HES simulations to calculate E_i of Eq. (21), which indicates the amount of CO_2 emitted,

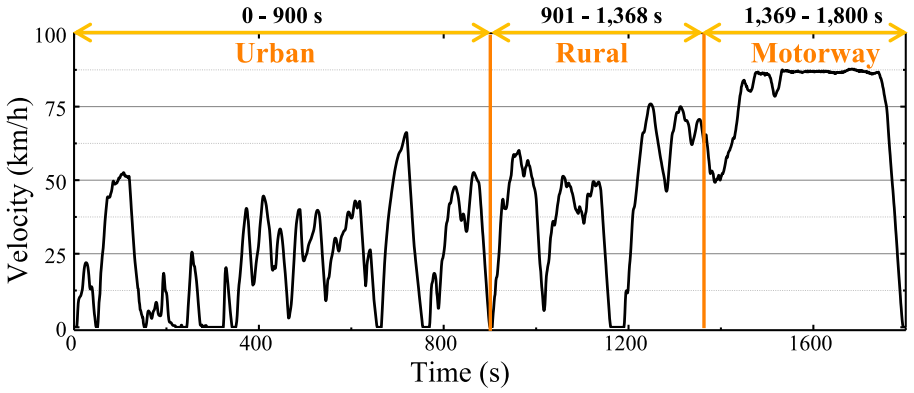

Fig. 11. K-WHVC driving cycle.

in grams, when a vehicle travels a distance of 1 km. Most of the vehicle data were collected from the database of NIER, the national regulatory body for vehicle emissions. The vehicle weight is determined by considering the loading weight to be half its maximum payload capacity. The weight of a passenger was assumed to be 65 kg. However, since the aerodynamic drag coefficient and rolling resistance coefficient were not available in this study, these variables were replaced with assumed values. The approximation method was used to estimate aerodynamic drag force (F_{air}) and rolling resistance force (F_R), which can be characterized using the following equations:

$$F_R = (0.005125 \bullet m + 17.601) \bullet g \tag{22}$$

$$F_{air} = (0.002625 \bullet A - 0.0006299) \bullet v^2 \tag{23}$$

Here, m is the vehicle weight [kg], g is the gravitational acceleration [m/s^2], A is the frontal area of the vehicle [m^2], and v is the vehicle speed [m/s].

Eqs. (22) and (23) have been used for fuel consumption estimation of HDVs in Japan (The Energy Conservation Center, 2005). Since this method requires only simple vehicle specifications such as vehicle weight and frontal area, it can be a practical alternative when the resistance coefficients are not available.

For driving cycle, the Korean-World Harmonized Vehicle Cycle (K-WHVC, Fig. 11) and weighting factors depending on vehicle types (Table 2) were used, which is the standard driving cycle for CO_2 emission certification of HDVs in Korea. Park et al. (2013) developed the K-WHVC and weighting factors based on the real road driving test of five types of HDVs (city bus, express bus, heavy-duty truck, extra-large truck, tractor) in Korea. In order to investigate the driving characteristics of HDVs, they collected speed, acceleration, pedal position, engine speed, and engine torque data by installing a CAN logger and vehicle speed recorder on the vehicles. They statistically analyzed the correlation between the driving patterns of Korean HDVs and existing driving cycles such as WHVC, ARB transient cycle, US 55 mph cycle, US 65 mph cycle, Japanese urban cycle, Japanese inter urban cycle, and other Korean driving cycles. Through the correlation analysis, they concluded that the WHVC is the most proper to represent the driving patterns of Korean HDVs among the existing driving cycles. However, several fully loaded heavy-duty trucks could not easily follow the target speed and rapid acceleration of the WHVC due to a lack of vehicle performance. When a vehicle cannot follow the target speed of the driving cycle, it is difficult to adequately assess the fuel consumption and CO_2 emissions of the vehicle. Therefore, Park et al. proposed a K-WHVC that partially relieved the acceleration of the WHVC. In addition, they developed weighting factors to represent various driving pattern of HDVs, which are shown in Table 2. The K-WHVC consisted of three phases that represent velocity pattern in urban, rural and motorway areas. Park et al. developed the optimal weighting factors that increased the correlation between K-WHVC and actual driving characteristics depending on vehicle types. By applying weighting factors depending on vehicle types, it is possible to properly consider the various driving patterns of HDVs. The velocity profile of the K-WHVC is illustrated in Fig. 11. The K-WHVC is a flat driving mode for which the road slope is set to zero. The average velocities of the urban, rural and motorway phases are 22, 44, and 77 km/h, respectively. In this study, K-WHVC and driving cycle weighting factors of Table 2 were used to calculate the E_i of Eq. (21).

2.4.2. Vehicle mileage and registration statistics

As shown in Eq. (21), CO_2 emissions from 2015 to 2020 were calculated by multiplying the simulation results by the annual mileage and the number of vehicles. Specifications of 375 vehicles were used as HES input to calculate E_i, and it was assumed that E_i were constant from 2015 to 2020. Table 3 shows the vehicle kilometer traveled (VKT) statistics by vehicle types from 2015 to 2020, published annually by the Korea Transportation Safety Authority (Korea Transportation Safety Autority, 2021).

The number of HDVs from 2015 to 2020 are shown in Table 4. HDVs are classified into trucks, tractors, and buses. Trucks are divided into medium-duty trucks and heavy-duty trucks according to their payload capacity. Trucks with a payload capacity of more than five tons are classified as heavy-duty trucks. The payload capacity of medium-duty trucks is between one and five tons. Since the trucks smaller than medium-duty trucks are classified as LDVs, they were not considered in this study. Buses are classified as city buses, inter-city buses, express buses, and ordinary buses depending on their use. The term ‘ordinary bus’ refers to the rest of the buses excluding city buses, inter-city buses, and express buses. Ordinary buses are further classified into medium-duty ordinary bus and heavy-duty ordinary buses according to their passenger capacity, length, width, and height. The total number of HDVs increased by about 5.2% from 847,616 in 2015 to 891,667in 2020. The HDVs are buses, trucks, and tractors and which account for 18%, 78%, and 4%, respectively. In Korea, most of HDVs use diesel and natural gas as a fuel, and the proportion of other fuels is very low (MOLIT, 2021). Specifically, 96.4% of HDVs are equipped with diesel engines and the remaining of HDVs are mostly compressed natural gas (CNG)-powered city buses.

Table 2
Diving cycle weight factors of K-WHVC.

Vehicle type		Driving cycle weighting factor (Urban: Rural: Motorway)
Truck, Tractor	Payload capacity $\leq$ 5 ton	2: 4: 4
	5 ton $<$ Payload capacity $\leq$ 25 ton	1.5: 3.5: 5
	25 ton $<$ Payload capacity	1: 3: 6
City bus		9: 1: 0
Ordinary bus		1: 2: 7

Table 3
Korean vehicle kilometers traveled statistics from 2015 to 2020.

Types	Vehicle kilometers traveled (km/day)					
	2015	2016	2017	2018	2019	2020
Medium-duty truck	51.4	51.3	51.7	49.3	46.5	50.6
Heavy-duty truck	134.4	134.5	137.9	135.7	134.8	133.1
Tractor	216.7	221.7	228.4	224.2	225.3	220.7
Medium-duty bus	44	45	44.5	43.9	43.4	40.2
Heavy-duty bus	191.1	193.1	195	193.3	191.4	173.9

Table 4
Korean vehicle registration statistics from 2015 to 2020.

Vehicle Types	The number of vehicles					
	2015	2016	2017	2018	2019	2020
Medium-duty truck	416,128	421,495	427,174	429,711	427,845	425.190
Heavy-duty truck	246,163	254,545	262,945	267,610	269,099	274.079
Tractor	36,068	37,943	38,619	38,795	38,751	39.232
City bus	36,483	38,955	40,877	42,246	43,137	42,182
Inter-city express bus	69,016	68,549	67,501	65,903	65,513	65,594
Medium-duty ordinary bus	26,143	26,177	26,667	26,764	26,729	26,993
Heavy-duty ordinary bus	17,615	18,308	19,047	19,619	19,899	19,397
Total	847,616	865,972	882,830	890,648	890,973	891,667

3. Results and discussion

3.1. HES validation using experimental data

This section describes the model validation results using experimental data. For validation of HES, three calculated variables (engine speed, engine torque, and CO_2 emissions) of thirteen HDVs were compared with experimental data. In addition to the CO_2 emissions, which are the final simulation results, engine speed and engine torque are the main operating variables representing the dynamic conditions of a vehicle. The time-based comparison results of engine speed, engine torque and CO_2 emissions of each vehicle are shown in Supplementary Fig. A.3 to A.12. Although some differences were observed between the calculated and experimental values, the overall prediction accuracy was satisfactory. The prediction errors were mainly caused by the difference between the actual shift timing and the simulated shift timing. Since the HES uses the predefined shifting threshold (normalized engine speed and engine torque) that cannot be modified by users, it is difficult to perfectly predict the shift timing of an actual vehicle. Excluding errors in some sections, the engine speed prediction accuracy was satisfactory. Supplementary Fig. A.3 to A.12 show that the simulation model accurately predicted experimental engine speed, engine torque, and CO_2 emissions.

Table 5
Comparison of experimental and simulation results of CO_2 emissions.

NO	Experimental CO_2 (g/km)	Simulation CO_2 (g/km)	Relative error (%)
Case 1-1	374.0	377.0	+0.8
Case 1-2	359.6	377.0	+4.8
Case 1-3	398.1	377.0	−5.3
Case 2	482.5	503.7	+4.4
Case 3-1	507.2	546.4	+7.7
Case 3-2	568.1	546.4	−3.8
Case 4-1	779.1	742.9	−4.7
Case 4-2	723.0	742.9	+2.7
Case 5-1	597.0	602.4	+0.9
Case 5-2	594.0	602.4	+1.4
Case 5-3	593.7	602.4	+1.5
Case 6	504.7	488.7	−3.2
Case 7	646.2	610.9	−5.5
Case 8	895.5	831.8	−7.1
Case 9	947.8	887.0	−6.4
Case 10	920.3	843.2	−8.4
Case 11	788.5	746.4	−5.3
Case 12	833.6	754.3	−9.5
Case 13	799.5	773.2	−3.3
Mean absolute Error (%): 4.6%			

Table 5 summarizes the experimental and simulation results relating to CO_2 emissions, and Fig. 12 illustrates the correlations between simulation results and experimental results. The reference line shows the ideal correlation, where the simulation results and the actual values match exactly. The mean absolute error in all cases is 4.6% and R^2 value is 0.9797, indicating that the simulation model has high CO_2 prediction accuracy. The mean absolute error between the chassis dynamometer test (Cases 1 through 5) and simulation model is 3.5%. Real road driving data-based mean absolute error (Cases 6 through 13) is 6.1%, which is higher that the chassis dynamometer-based validation results.

The main reason for the higher CO_2 error in real road test-based verification than in chassis dynamometer-based verification is due to the air drag and rolling resistance coefficients. In this study, approximate coefficients, as presented in Eqs. (22) and (23), were utilized as input for the simulation and as the setup value for the driving resistance of the chassis dynamometer test. Therefore, the driving resistance conditions for the simulation and chassis dynamometer test are the same. However, since the approximate coefficients differs from the actual resistance coefficients, there was a relatively high CO_2 error for real road test-based validation. In addition, compared to the chassis dynamometer test conducted under controlled conditions in a laboratory, the real road driving test is affected by various factors such as weather and traffic conditions. Due to these disturbances of real road driving test, the prediction accuracy of HES for real road-driving CO_2 emissions was lower than that of the chassis dynamometer test-based CO_2 emissions.

3.2. Comparison of HES and European simulation model VECTO

VECTO is the simulation program for CO_2 certification of European HDVs (Fontaras et al., 2013b; European Commission, 2017). VECTO calculates the fuel consumption and CO_2 emissions of HDVs based on longitudinal vehicle dynamics. The backward-looking approach was used for the development of VECTO. In the driver module of VECTO, the forward-looking approach is also used to implement realistic vehicle speed control such as eco-roll, look ahead coasting, and control of over-speeding. This chapter describes the similarities and differences between the HES and VECTO. The simulation results of VECTO and HES using the same input data were compared.

Both HES and VECTO calculate CO_2 emissions and fuel consumptions by calculating the energy consumption of individual components of a vehicle. The required engine power is calculated by adding up all energy consumed by each component. Based on the calculated engine power, fuel consumption is interpolated from a fuel consumption map. CO_2 emissions were then calculated using the carbon balance method. The energy balance of the engine for HES and VECTO can be described as follows:

Energy balance of HES

$$P_{engine} = P_{air} + P_{RR} + P_{acc} + P_{grad} + P_{enginertia} + P_{gbxloss} + P_{retloss} + P_{axleloss} + P_{wheelinertia} + P_{brake} + P_{aux} \quad (24)$$

Energy balance of VECTO

$$P_{engine} = P_{air} + P_{RR} + P_{acc} + P_{grad} + P_{enginertia} + P_{gbxloss} + P_{retloss} + P_{axleloss} + P_{wheelinerita} + P_{brake} + P_{aux} + P_{gbxinertia} + P_{PTO} + P_{clutchloss} \quad (25)$$

Here, P_{engine} is the engine power [W], P_{air} is the power loss due to the air drag [W], P_{RR} is the power loss due to the rolling resistance [W], P_{acc} is the power loss or gain due to the vehicle acceleration [W], P_{grad} is the power loss or gain due to road grad [W], $P_{enginertia}$ is the power loss or gain due to the engine inertia [W], $P_{gbxloss}$ is the transmission loss at the gear box [W], $P_{retloss}$ is the power loss at the retarder [W], $P_{axleloss}$ is the transmission loss at the axle gear [W], $P_{wheelinertia}$ is the power loss or gain due to the inertia of wheels [W], P_{brake} is the power loss due to braking [W], P_{aux} is the power consumption of auxiliary devices [W], $P_{gbxinertia}$ is the power loss due to the inertia of gearbox [W], P_{PTO} is the power consumption of PTO (Power Take Off) devices [W], and $P_{clutculoss}$ is the power loss due to the clutch disengagement [W].

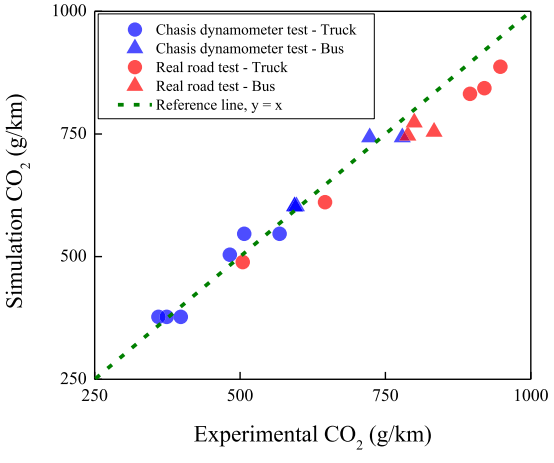

Fig. 12. CO_2 emission correlation between simulation results and experimental results.

The engine power of HES and VECTO are calculated by considering the sub-components of the vehicle. Most of the major sub-components are considered in both the simulation models. However, VECTO considers more sub-components to calculate the energy consumption as compared to HES. The $P_{gbxinertia}$, P_{PTO}, and $P_{clutchloss}$ are only considered in the energy balance of VECTO in Eq. (25). Gearbox inertia, additional energy consumption of PTO devices, and declutching events are not considered in HES.

The simulation results of HES and VECTO were compared. Simulation calculations of HES and VECTO were performed using the example data of VECTO (European Commission, 2021). The vehicle specifications for simulation input are shown in Supplementary Table A.1. For comparative analysis, we used regional delivery cycle (Fig. A.13) for CO_2 calculation. The regional delivery cycle is distance-based mission profile that defined by the target speed and altitude according to the traveled distance. During the VECTO simulation, the target speed of the regional delivery cycle is adjusted by the driver module depending on the vehicle performance. In contrast, HES uses a time-based vehicle speed profile for CO_2 calculation. Therefore, in order to compare the simulation results of VECTO and HES under the same driving conditions, the velocity and altitude data of VECTO results were used as input data for HES. In this study, the simulation results for vehicle speed between HES and VECTO were almost identical. The time-based energy consumption rate of each sub-component is presented in Supplementary Fig. A.14 to A.24.

Supplementary Fig. A.24 shows that, despite VECTO performing upward and downward gear shifts more sensitively than HES and having a higher frequency of gear shifts, overall gear shifting tendencies are similar between HES and VECTO. Fig. 13 illustrates the calculated engine power of HES and VECTO, which is the sum of the energy consumption of all sub-components. Since both HES and VECTO calculate fuel consumptions using engine speed and an engine torque-based interpolation function, the prediction accuracy of the engine operating condition is directly related to the prediction accuracy of fuel consumption and CO_2 emission. The comparison results of Fig. 13 shows that the calculated engine power of VECTO and HES results are quite similar.

Fuel consumption rates of HES and VECTO are compared in Fig. 14. The difference in the cumulative fuel consumption calculated by HES and VECTO is 1.4%. This result indicates that the fuel consumption prediction accuracy of HES and VECTO is similar when using the same input data.

To quantitatively analyze the prediction accuracy of the HES and VECTO, 21 simulations were performed for both HES and VECTO. Three types of vehicles (Class 5 tractor, Class 9 rigid truck, Class 2 rigid truck) were used to perform the simulation. These vehicles were provided as examples data of VECTO and are included in the downloadable software package of VECTO (European Commission, 2021). Two driving cycles of VECTO (long haul, regional delivery) and K-WHVC were used for the simulation. The simulation conditions and the calculated CO_2 emissions are shown in Table 6. The mean absolute CO_2 error between HES and VECTO results was 1.59%, and the coefficient of determination (R^2) between calculated CO2 values using HES and VECTO is 0.9958. The R^2 value, which is close to 1, indicates that the correlation between the CO_2 emission results of HES and VECTO was high.

The main cause of error between HES and VECTO is the difference in rolling resistance force. As shown in Eq. (2), HES use simple equation to calculate rolling resistances. In contrast, VECTO applied corrections to calculate rolling resistance as sown in Fig. A. 15. This difference account for a major part of the total CO_2 value discrepancy between HES and VECTO. When we recalculated the CO_2 emissions of HES using manually corrected RRC values based on the rolling resistance model of VECTO, which is shown in Table A.2, the deviation between the CO_2 calculation results of HES and VECTO was significantly reduced (average CO2 error: 0.94%).

3.3. CO_2 emissions from heavy-duty vehicles from 2015 to 2020 in Korea

Based on the method explained in subchapter 2.4, simulation results of 375 vehicles and statistical data were used to assess annual CO_2 emissions from HDVs from 2015 to 2020. Fig. 15 shows the annual CO_2 emissions from 2015 to 2020. In 2015, the total CO_2 emissions from HDVs was 20.5 million tons, which is the 2.96% of domestic GHG emission and 21.76% of transport GHG emissions (Greenhouse Gas Inventory and Research Center, 2019). The CO_2 emissions in 2020 were 22.5 million tons, an increase of 9.8% when compared to 2015. The average annual increase in the rate of CO_2 emissions was 1.88%. In 2020, heavy-duty trucks and medium-duty trucks accounted for 23% and 43% of the total HDV emissions, respectively. Although the number of heavy-duty trucks was lower than that of medium-duty trucks as shown in Table 3, the total CO_2 emissions from a heavy-duty truck were higher than that of a medium-duty truck due to the higher CO_2 emission rate (g/km) and higher VKT. CO_2 emissions from buses and tractors account for 23% and 11% of the total HDV emissions, respectively.

The CO_2 emissions from HDVs based on the type of fuel used are shown in Fig. 16. In Korea, 96.4% of HDVs are diesel-powered vehicle, and the remaining HDVs are mostly CNG-powered vehicles. The proportion of other fuels is insignificant in the HDV market in Korea. The CO_2 estimation results show that most CO_2 emissions were emitted from diesel HDVs, and only 6.8% of CO_2 was emitted from CNG HDVs in 2020. Although the proportion of CNG HDVs in Korea is 3.6%, the CO_2 emissions of CNG HDVs account for 6.8% of the total CO_2 emissions of HDVs. Since most of CNG HDVs are used for city buses as public transportation, their annual mileage is higher than other HDVs (Table 3, heavy-duty bus). In addition, CO2 emissions (g/km) for city driving are generally higher than for other driving patterns such as motorway driving, resulting in relatively high CO2 emissions of CNG HDVs.

4. Conclusion

HES was developed for CO_2 emission certification for HDVs in Korea. Mandatory CO_2 standards for HDVs is expected to be implemented from 2026, and HDV manufacturers are required to submit CO2 calculation data of HDVs sold in Korea using the HES program. This study addresses the development of HES program, including description of modeling methods and validation of CO_2 prediction accuracy.

The prediction accuracy of HES was validated by comparing the simulation results with experimental results. The average CO_2

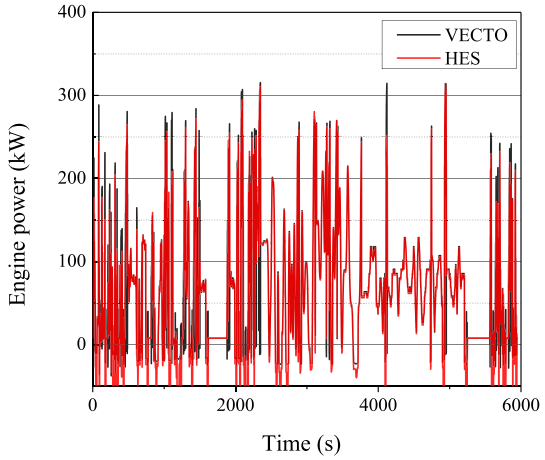

Fig. 13. Calculated engine power of HES and VECTO simulation.

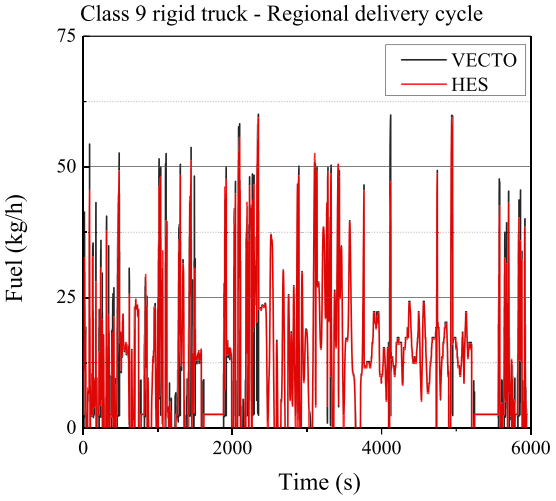

Fig. 14. Fuel consumption of HES and VECTO simulation.

emission error between the chassis dynamometer test and simulation results of was 3.5%, and the real road driving data-based average CO_2 emission error was 6.1%. In contrast to the chassis dynamometer test, which was performed in the laboratory under controlled conditions, the real road driving test was affected by various factors such as the uncertainty of driving resistance coefficient, environment, and traffic conditions. Due to these disturbances in the real road driving test, the CO_2 prediction error for real driving conditions is slightly higher than the chassis dynamometer test. The average CO_2 prediction error of all the cases (total 19 vehicle tests: 11 chassis dynamometer tests and 8 real road driving tests) is 4.6%, indicating that the CO_2 prediction accuracy of HES is high.

In addition to the validation using experimental data, the model structure and simulation results of HES were compared with that of VECTO. HES and VECTO calculated the CO_2 emissions and fuel consumptions by calculating the energy consumption of individual components of the vehicle. Both programs consider the following components in simulations: aerodynamic drag, rolling resistance, acceleration force, inclination force, engine inertia, transmission loss at gear box, transmission loss at the retarder, transmission loss at the axle gear, wheel inertia, and auxiliary power consumption. However, gearbox inertia, power consumption of PTO devices, and transmission loss at the clutch are only considered in VECTO. Although slight differences were observed in the results of the calculation for each sub-component, the total energy consumption of HES and VECTO were similar. For comparative analysis, 21 cases of simulations were performed for both HES and VECTO. Vehicle information for three types of vehicles (Class 5 tractor, Class 9 rigid truck, Class 2 rigid truck) were used for simulation input. The average CO_2 error of 21 cases of simulations was 1.77%., indicating the correlation of HES and VECTO was high.

CO_2 emissions from Korean HDVs were estimated by integrating simulation results and national statistical data. The total CO_2 emissions from HDVs in 2015 was 20.5 million tons, which is 2.96% of the national GHG emissions and 21.76% of transport GHG emissions. In 2020, 22.5 million tons of CO_2 was emitted from HDVs, an increase of 9.8% compared to 2015.

Table 6
CO_2 calculation results of HES and VECTO using the same input data.

Vehicle type	Driving cycle	Vehicle weight	VECTO results: CO_2 (g/km)	HES results: CO_2 (g/km)	Relative error (%)
Class 5 Tractor	Long Haul	18,329 kg	691	674	2.51
12.7 L engine		35,029 kg	909	898	1.22
	Regional Delivery	18,329 kg	734	716	2.46
		28,629 kg	913	897	1,73
	K-WHVC	18,329 kg	789	810	2.18
		35,029 kg	1200	1187	1.09
		28,629 kg	1030	1039	0.89
Class 9	Long Haul	19,500 kg	767	743	3.13
Rigid truck		36,200 kg	969	957	1.14
7 L engine	Regional Delivery	12,900 kg	603	590	2.24
		18,600 kg	689	679	1.40
	K-WHVC	18,600 kg	760	731	3.81
		22,050 kg	820	803	2.10
		12,900 kg	627	616	1.71
Class 2	Long Haul	11,274 kg	691	676	2.22
Rigid truck		19,811 kg	801	798	0.32
6.8 L engine	Regional Delivery	7,174 kg	526	526	0.07
		9,590 kg	568	569	0.17
	K-WHVC	11,274 kg	555	565	1.77
		7,174 kg	462	463	0.28
		9,590 kg	517	521	0.69

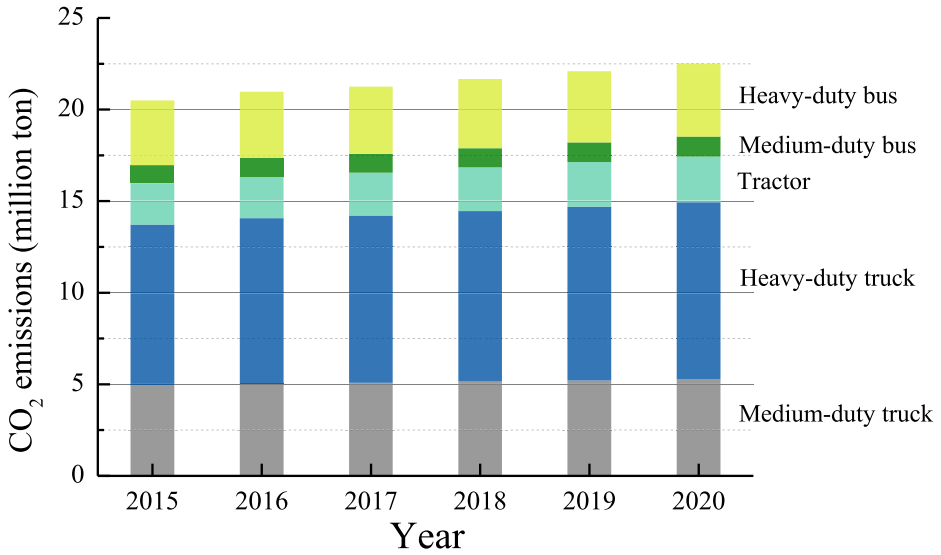

Fig. 15. Annual CO_2 emissions from HDVs from 2015 to 2020 in Korea.

This study describes the CO_2 estimation method for HDVs based on vehicle dynamics and system modelling. Since the simulation model calculated CO_2 emissions using input data, which were measured from sub-component testing, the quality of the input data had a significant impact on CO_2 prediction accuracy. The uncertainty of input data might cause unintended errors in CO_2 estimation. To rigorously validate CO_2 prediction accuracy, it is necessary to consider the impact of input data quality on CO_2 prediction accuracy. In addition, HES program cannot calculate the CO2 emissions of hybrid electric vehicle. In order to calculate the CO2 emissions of hybrid electric vehicles, simulation model have to calculate the energy consumptions of electric motors. However, it is difficult to develop a representative hybrid vehicle model because the energy consumption of the electric motor is highly dependent on the powertrain control system. Therefore, future work should include a CO_2 certification methodology for heavy-duty hybrid vehicles.

CRediT authorship contribution statement

Jigu Seo: Writing – original draft, Investigation, Methodology. **Sungwook Park:** Writing – review & editing, Supervision.

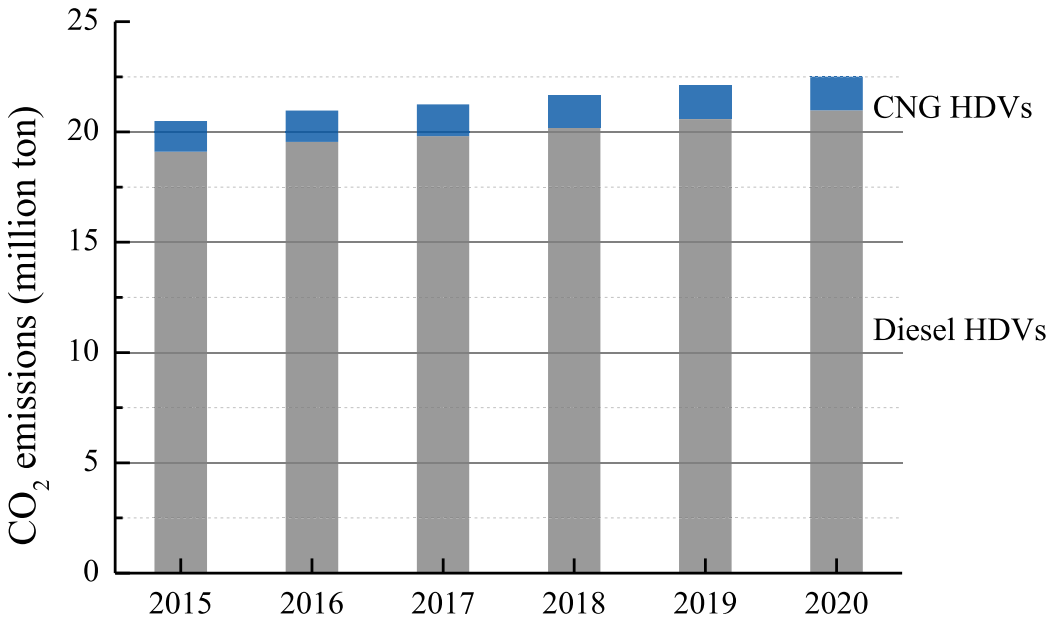

Fig. 16. Annual CO_2 emissions from HDVs by fuel type (diesel and CNG).

Declaration of Competing Interest

The authors declare that they have no known competing financial interests or personal relationships that could have appeared to influence the work reported in this paper.

Data availability

Data will be made available on request.

Acknowledgement

This work was supported by BK21 FOUR Program.

Appendix A. Supplementary data

Supplementary data to this article can be found online at https://doi.org/10.1016/j.trd.2023.103774.

References

Akita, Masanobu, 2014. Real-time fuel consumption measurement using raw exhaust flow meter and zirconia AFR sensor. Featur. Artic. Appl. 42, 91–96. https://static.horiba.com/fileadmin/Horiba/Company/About_HORIBA/Readout/R42E/R42E_14_091_01.pdf.

Beevers, S.D., Carslaw, D.C., 2005. The impact of congestion charging on vehicle speed and its implications for assessing vehicle emissions. Atmos. Environ. 39 (36), 6875–6884. https://doi.org/10.1016/j.atmosenv.2005.08.021.

Bernstein, Lenny, Peter Bosch, Osvaldo Canziani, Zhenlin Chen, Renate Christ, Ogunlade Davidson, William Hare, Saleemul Huq, David J Karoly, Vladimir Kattsov, 2008. Climate Change 2007 Synthesis Report: IPCC.

Carolien, Beckx, LI Panis, Torfs Rudi, Janssens Davy, Broekx Steven, 2007. The application of the simulation software vetess to evaluate the environmental impact of traffic measures. In: 10th Conference on Computers on Urban Planning and Urban Management.

The Energy Conservation Center, 2005. Final Report by Heavy Vehicle Fuel Efficiency Standard Evaluation Group, Heavy Vehicle Standards Evaluation Subcommittee, Energy Efficiency Standards Subcommittee of the Advisory Committee for Natural Resources and Energy. https://www.eccj.or.jp/top_runner/pdf/heavy_vehicles_nov2005.pdf.

Environmental Protection Agency, 2016. Greenhouse Gas Emissions and Fuel Efficiency Standards for Medium- and Heavy-Duty Engines and Vehicles—Phase 2. Federal Register / Vol. 81, No. 206.

EPA. GEM Phase2 V4.0. https://www.epa.gov/regulations-emissions-vehicles-and-engines/greenhouse-gas-emissions-model-gem-medium-and-heavy-duty#overview.

European Commission, 2017. Commission Regulation (EU) 2017/2400 of 12 December 2017 implementing Regulation (EC) No 595/2009 of the European Parliament and of the Council as regards the determination of the CO2 emissions and fuel consumption of heavy-duty vehicles and amending Directive 2007/46/EC of the European Parliament and of the Council and Commission Regulation (EU) No 582/2011. Off. J. Eur. Union.

European Commission, 2018. Commission Regulation (EU) 2018/956 OF THE EUROPEAN PARLIAMENT AND OF THE COUNCIL of 28 June 2018 on the monitoring and reporting of CO2 emissions from and fuel consumption of new heavy-duty vehicles. Off. J. Eur. Union.
European Commission, 2019. Commission Regulation (EU) 2019/1242 OF THE EUROPEAN PARLIAMENT AND OF THE COUNCIL of 20 June 2019 setting CO2 emission performance standards for new heavy-duty vehicles and amending Regulations (EC) No 595/2009 and (EU) 2018/956 of the European Parliament and of the Council and Council Directive 96/53/EC. Off. J. Eur. Union.
European Commission, 2021. VECTO v3.3.10.2401 download. https://ec.europa.eu/clima/eu-action/transport-emissions/road-transport-reducing-co2-emissions-vehicles/vehicle-energy_en.
Fontaras, Georgios, Martin Rexeis, Panagiota Dilara, Stefan Hausberger, Konstantinos Anagnostopoulos, 2013a. The development of a simulation tool for monitoring heavy-duty vehicle co 2 emissions and fuel consumption in europe. SAE Technical Paper.
Fontaras, Georgios, Martin Rexeis, Panagiota Dilara, Stefan Hausberger, Konstantinos Anagnostopoulos, 2013b. The development of a simulation tool for monitoring heavy-duty vehicle co 2 emissions and fuel consumption in europe. (2013-24-0150). 10.4271/2013-24-0150.
Gillespie, Thomas D., 1992. Fundamentals of vehicle dynamics.
Greenhouse Gas Inventory and Research Center, 2019. National greenhouse gas inventory report of Korea. https://www.gihoo.or.kr/portal/kr/community/data_view.do?p=1&idx=20302&column=&groupname=data&groupid=&f=1&q=.
Grubb, Michael, Christiaan Vrolijk, Duncan Brack, 1999. The Kyoto Protocol: a guide and assessment.
Gururaja, Prashanth, 2016. Evaluation of Coastdown Analysis Techniques to Determine Aerodynamic Drag of Heavy-Duty Vehicles. (2016-01-8151). 10.4271/2016-01-8151.
Hausberger, Stefan, 2009. Emission Factors from the Model PHEM for the HBEFA Version 3.
ISO 28580, 2009. Passenger Car, Truck, and Bus Tyres Methods of Measuring Rolling Resistance - Single Point Test and Correlation of Measurement Results. International Organisation for Standardization, Geneva, Switzerland.
Korea Transportation Safety Autority, 2021. Vehicle Mileage Statistics. http://www.kotsa.or.kr/tsk/rck/InqDetPTRTrafficSafety.do?bbsSn=5493&bbsCd=110&ctgCd=-1.
Lee, Hoon, Hoimyung Choi, Minje Park, Kyoungdoug Min, Nankyu Lee, Jinil Park, Jong-Hwa Lee, 2015. Development of a vehicle system model for the first medium- and heavy-duty commercial vehicle fuel efficiency standards in Korea (2015-01-2774). 10.4271/2015-01-2774.
Masson-Delmotte, V., Zhai, P., Pörtner, H.-O., Roberts, D., Skea, J., Shukla, P.R., Anna Pirani, W., Moufouma-Okia, C.P., Pidcock, R., 2018. Global warming of 1.5 C. IPCC Special Report 1 (5).
ME, 2019. Notification No.2030-399. Guidelines for the application of average energy consumption efficiency standards and greenhouse gas standards for medium and heavy-duty vehicles. https://www.law.go.kr/LSW/admRulLsInfoP.do?admRulSeq=2100000196337.
Miller, Josh, Li Du, Kodjak, Drew, 2017. Impacts of world-class vehicle efficiency and emissions regulations in select G20 countries. ICCT report: 24.
MOLIT, 2021. Korean vehicle registration statistics. https://stat.molit.go.kr.
MOTIE, ME, MOLIT, 2015. Notification No.2015-63. Test Methods for Vehicle Energy Efficiency, Greenhouse Gas Emissions, and Fuel Consumption. Last amendment April 8th 2015. https://www.law.go.kr/admRulLsInfoP.do?admRulSeq=2200000071752.
Newman, Kevin A, Paul Dekraker, Houshun Zhang, James Sanchez, Gururaja, Prashanth, 2015. Development of Greenhouse Gas Emissions Model (GEM) for Heavy- and Medium-Duty Vehicle Compliance. SAE Int. J. Commer. 8 (2015-01-2771, 388–309. 10.4271/2015-01-2771.
Pacejka, Hans, 2005. Tire and Vehicle Dynamics, Elsevier.
Pachauri, Rajendra K., Allen, Myles R., Barros, Vicente R., Broome, John, Cramer, Wolfgang, Christ, Renate, Church, John A., Clarke, Leon, Dahe, Qin, Dasgupta, Purnamita, 2014. Climate change 2014: synthesis report. Contribution of Working Groups I, II and III to the fifth assessment report of the Intergovernmental Panel on Climate Change, IPCC.
Park, Jinil, Lee, Jong-Hwa, Lee, Jongseop, 2013. Development of Driving Cycle for CO2 Emission Test of Heavy-Duty Vehicles. (2013-01-2520). 10.4271/2013-01-2520.
Pettersson, P., Jacobson, B., Bruzelius, Fredrik, Johannesson, P., Fast, L., 2020. Intrinsic differences between backward and forward vehicle simulation models. IFAC-PapersOnLine 53(2), 14292–14299. 10.1016/j.ifacol.2020.12.1368.
Rogelj, J., Den Elzen, M., Höhne, N., Fransen, T., Fekete, H., Winkler, H., Roberto Schaeffer, F.u., Sha, K.R., Meinshausen, M., 2016. Paris Agreement climate proposals need a boost to keep warming well below 2 C. Nature 534 (7609), 631–639. https://doi.org/10.1038/nature18307.
Seo, J., Park, J., Yunjung, O.h., Park, S., 2016. Estimation of total transport CO2 emissions generated by medium- and heavy-duty vehicles (MHDVs) in a sector of Korea. Energies 9 (8), 638.
Sharpe, Ben, Muncrief, Rachel, 2015. Literature review: real-world fuel consumption of heavy-duty vehicles in the United States, China, and the European Union. ICCT report.
Sharpe, Ben, Lutsey, Nic, Delgado, Oscar, Muncrief, Rachel, 2018. United States efficiency and greenhouse gas emission regulations for model year 2018-2027 heavy-duty vehicles, engines, and trailers. ICCT report.
Siskos, P., Moysoglou, Y., 2019. Assessing the impacts of setting CO2 emission targets on truck manufacturers: a model implementation and application for the EU. Transp. Res. A Policy Pract. 125, 123–138. https://doi.org/10.1016/j.tra.2019.05.010.
Sudin, Mohd Nizam, Abdullah, Mohd Azman, Shamsuddin, Shamsul Anuar, Ramli, Faiz Redza, Tahir, Musthafah Mohd, 2014. Review of research on vehicles aerodynamic drag reduction methods. Int. J. Mech. Mechatron. 14(02), 37-47. https://files.core.ac.uk/pdf/13518/235648507.pdf.
Sun, D., Zheng, Y., Duan, R., 2021. Energy consumption simulation and economic benefit analysis for urban electric commercial-vehicles. Transp. Res. Part D: Transp. Environ. 101, 103083 https://doi.org/10.1016/j.trd.2021.103083.
Triantafyllopoulos, G., Dimaratos, A., Ntziachristos, L., Bernard, Y., Dornoff, J., Samaras, Z., 2019. A study on the CO2 and NOx emissions performance of Euro 6 diesel vehicles under various chassis dynamometer and on-road conditions including latest regulatory provisions. Sci. Total Environ. 666, 337–346. https://doi.org/10.1016/j.scitotenv.2019.02.144.
Tutuianu, M., Bonnel, P., Ciuffo, B., Haniu, T., Ichikawa, N., Marotta, A., Pavlovic, J., Steven, H., 2015. Development of the World-wide harmonized Light duty Test Cycle (WLTC) and a possible pathway for its introduction in the European legislation. Transport. Res. Part D-Transport. Environ. 40, 61–75. https://doi.org/10.1016/j.trd.2015.07.011.
Yang, Zifei, Bandivadekar, Anup, 2017. Light-duty vehicle greenhouse gas and fuel economy standards. ICCT report: 16.
Zacharof, Nikiforos, Fontaras, Georgios, Grigoratos, Theodoros, Ciuffo, Biagio, Savvidis, Dimitrios, Delgado, Oscar, Felipe Rodriguez, J., 2017. Estimating the CO 2 emissions reduction potential of various technologies in European trucks using VECTO simulator. (2017-24-0018). 10.4271/2017-24-0018.
Zacharof, N., Fontaras, G., Ciuffo, B., Tansini, A., Prado-Rujas, I., 2021. An estimation of heavy-duty vehicle fleet CO2 emissions based on sampled data. Transp. Res. Part D: Transp. Environ. 94, 102784 https://doi.org/10.1016/j.trd.2021.102784.